Journal of Cerebral Blood Flow & Metabolism (2012) 32, 2122–2134

www.jcbfm.com

JCBFM Open

Altered neurochemical profile after traumatic brain injury: ^{1}H-MRS biomarkers of pathological mechanisms

Janna L Harris[1], Hung-Wen Yeh[2], In-Young Choi[1,3], Phil Lee[1,4], Nancy E Berman[5], Russell H Swerdlow[3,4,6], Sorin C Craciunas[7] and William M Brooks[1,3,4]

[1]*Hoglund Brain Imaging Center, University of Kansas Medical Center, Kansas City, Kansas, USA;* [2]*Department of Biostatistics, University of Kansas Medical Center, Kansas City, Kansas, USA;* [3]*Department of Neurology, University of Kansas Medical Center, Kansas City, Kansas, USA;* [4]*Department of Molecular and Integrative Physiology, University of Kansas Medical Center, Kansas City, Kansas, USA;* [5]*Department of Anatomy and Cell Biology, University of Kansas Medical Center, Kansas City, Kansas, USA;* [6]*Department of Biochemistry and Molecular Biology, University of Kansas Medical Center, Kansas City, Kansas, USA;* [7]*Bagdasar-Arseni Hospital, Neurosurgery Unit IV, Carol Davila University of Medicine, Bucharest, Romania*

Specific neurochemicals measured with proton magnetic resonance spectroscopy (^{1}H-MRS) may serve as biomarkers of pathological mechanism in the brain. We used high field *in vivo* ^{1}H-MRS to measure a detailed neurochemical profile after experimental traumatic brain injury (TBI) in rats. We characterized neurochemical changes in the contused cortex and the normal-appearing perilesional hippocampus over a time course from 1 hour to 2 weeks after injury. We found significant changes in 19 out of 20 neurochemicals in the cortex, and 9 out of 20 neurochemicals in the hippocampus. These changes provide evidence of altered cellular metabolic status after TBI, with specific compounds proposed to reflect edema, excitotoxicity, neuronal and glial integrity, mitochondrial status and bioenergetics, oxidative stress, inflammation, and cell membrane disruption. Our results support the utility of ^{1}H-MRS for monitoring cellular mechanisms of TBI pathology in animal models, and the potential of this approach for preclinical evaluation of novel therapies.
Journal of Cerebral Blood Flow & Metabolism (2012) **32,** 2122–2134; doi:10.1038/jcbfm.2012.114; published online 15 August 2012

Keywords: animal models; brain trauma; cell death mechanisms; MR spectroscopy; neurochemistry

Introduction

Despite the major public health implications of traumatic brain injury (TBI), treatments to limit brain damage and promote recovery remain elusive. The initial physical impact of TBI unleashes numerous pathological cellular processes—including inflammation, oxidative stress, mitochondrial dysfunction, excitotoxicity, edema, and hypoxia—that unfold over a period of hours to weeks, each contributing to brain tissue damage. The failure of clinical trials is due in part to this complexity of TBI pathology, and to the absence of biomarkers that reflect specific pathophysiological mechanisms in individual patients (Loane and Faden, 2010).

Mounting evidence indicates that specific neurochemicals resolved with *in vivo* proton magnetic resonance spectroscopy (^{1}H-MRS) may serve as biomarkers of injury mechanism. For example, several studies in TBI have found decreased N-acetylaspartate (NAA) suggesting neuronal mitochondrial dysfunction and/or neurodegeneration, elevated lactate (Lac) suggesting hypoxia, and elevated choline (Cho) and *myo*-inositol (Ins) implicating membrane breakdown and/or inflammation (Brooks *et al*, 2001; Marino *et al*, 2011). Other studies in human survivors of TBI have shown altered glutamine and glutamate (Babikian *et al*, 2006; Shutter *et al*, 2004). Moreover,

Correspondence: Dr JL Harris, Hoglund Brain Imaging Center, University of Kansas Medical Center, Mail Stop 1052, 3901 Rainbow Boulevard, Kansas City, KS 66160, USA.
E-mail: jharris2@kumc.edu
This study was supported in part by the National Institutes of Health (UL1 TR000001 to Frontiers: The Heartland Institute for Clinical and Translational Research at the University of Kansas Medical Center; P30 HD002528 to the Kansas Intellectual and Developmental Disabilities Research Center; P30 AG035982 to the University of Kansas Alzheimer's Disease Center; R01 AG031140 to Dr Berman; and R03 NS077852 to Dr Swerdlow) and a University of Kansas Lied Endowed Basic Science grant to Dr Brooks. The Hoglund Brain Imaging Center is supported by a generous gift from Forrest and Sally Hoglund.
Received 17 February 2012; revised 5 June 2012; accepted 13 July 2012; published online 15 August 2012

changes in certain neurochemicals that are visible with ^{1}H-MRS correlate with injury severity (Garnett *et al*, 2000) and are linked with cognitive outcomes in TBI survivors (Brooks *et al*, 2000; Holshouser *et al*, 2006), suggesting that MRS might be useful for clinical management. Results from spectroscopic studies in children are generally consistent with those in adults (Ashwal *et al*, 2000, 2004). More recently, ^{1}H-MRS studies in mild TBI have found altered brain neurochemistry (Gasparovic *et al*, 2009; Govind *et al*, 2010; Vagnozzi *et al*, 2010).

To date, ^{1}H-MRS investigations of animal models of TBI have also been limited to seven or fewer brain chemicals (Lescot *et al*, 2010; Schuhmann *et al*, 2003; Xu *et al*, 2011). Nonetheless, animal studies provide an opportunity to link spectroscopic findings with specific pathological mechanisms. Schuhmann *et al* (2003) completed an extensive time course to link neurochemical changes with histological findings and Xu *et al* (2011) have shown that MRS findings parallel structural injury implicated by diffusion tensor magnetic resonance imaging (MRI).

With high field strength scanners and advanced magnetic resonance techniques, ^{1}H-MRS can quantify >18 metabolites in the rodent brain *in vivo* (Pfeuffer *et al*, 1999; Tkac *et al*, 2003). This detailed 'neurochemical profile' of cellular metabolic status has been analyzed in rodent models of neurodegenerative disease and ischemic injury (Lei *et al*, 2009; Zacharoff *et al*, 2012) but not in TBI. Therefore, our goal in the current study was to assess the evolution of a comprehensive neurochemical profile after TBI, and to determine whether ^{1}H-MRS could detect changes in putative biomarkers of injury mechanism.

We used high field *in vivo* ^{1}H-MRS to examine the effects of a controlled cortical impact (CCI) targeting the sensorimotor cortex in rats. Controlled cortical impact is a widely used model that recapitulates many features of contusive brain injury seen in humans, including disruption of the blood–brain barrier, edema, hemorrhage, glial activation, and neurodegeneration (Chen *et al*, 2003; Dixon *et al*, 1991; Soblosky *et al*, 1996). The study covered a time course from 1 hour to 2 weeks after TBI, which allowed us to track the evolution of neurochemical changes from early acute through more chronic stages of TBI pathology in the same subjects. Behavioral testing and T_2-weighted MRI verified that the injury was highly consistent across animals and of a comparable severity to previous studies in the field (Chen *et al*, 2003; Hall *et al*, 2008). Proton magnetic resonance spectroscopy was acquired in two brain regions: a voxel located at the site of the developing cortical contusion and a voxel in adjacent normal-appearing hippocampus. This approach provided an opportunity to compare the neurochemical profile of severely damaged brain tissue destined to degenerate into an overt cyst with the profile of normal-appearing brain tissue that did not develop an MRI-visible lesion. This study substantially broadens the spectrum of neurochemicals that might serve as noninvasive biomarkers in TBI, and lays a foundation for future assessments of novel therapeutics.

Materials and methods

Animals

Twelve male Fisher rats (F344; Charles River, Wilmington, MA, USA) were used for the TBI study. Rats were 63 to 70 days old (175 to 200 g) when they received TBI. Animals were housed in pairs on a 12-hour light-dark cycle with free access to standard rat chow and water. All protocols were approved by the University of Kansas Animal Care and Use Committee and are consistent with standards of animal care set forth in the guidelines of the US Public Health Service Policy on Humane Care and Use of Laboratory Animals.

Controlled Cortical Impact

Animals were anesthetized with isoflurane (4% induction, 2% to 3% maintenance). Their heads were shaved and immobilized in a stereotaxic frame. Before surgery, a long-acting local analgesic (0.25% bupivacaine subcutaneously) was administered at the site of incision. Body temperature was maintained during surgery with a heating pad. A single midline incision exposed the skull, and the scalp and underlying connective fascia were reflected. A 6-mm-diameter craniotomy was formed with a Michele trephine over the right sensorimotor cortex, directly lateral to bregma and centered midway between bregma and the temporal ridge. Special care was taken not to disrupt the dura or associated vasculature during craniotomy. Cortical impact was delivered to the dural surface with an electromagnetically controlled impact device mounted on a stereotaxic manipulator (Leica; Saint Louis, MO, USA; impactor tip size = 5 mm; velocity = 3.5 m/s; depth = 2 mm; contact time = 300 ms). After impact the integrity of the dura mater was confirmed visually and the incision sutured closed. Animals were then transferred immediately to the adjacent MRI suite under continuous anesthesia.

In Vivo Magnetic Resonance Imaging and Spectroscopy

The MRI and ^{1}H-MRS scans were performed before TBI (within 2 weeks) and after TBI on Day 0 (D0), D1, D3, D7, and D14. All magnetic resonance assessments were performed in a 9.4-Tesla horizontal bore magnet (Varian Inc, Palo Alto, CA, USA) equipped with a 12-cm gradient coil (40 G/cm, 250 μs) and interfaced to a Varian INOVA console. During imaging, anesthesia was maintained with 1.5% to 3% isoflurane in a 70/30 mixture of air/O_2 delivered via nosecone to maintain a respiration rate of 40 to 80 cycles/min. Respiration was monitored with a pressure pad (SA Instruments, Stony Brook, NY, USA). Animals were placed on a heating pad in the scanning cradle, and body temperature monitored rectally was maintained at 37°C via feedback control (Cole Parmer, Vernon Hills, IL, USA).

Coronal and sagittal gradient echo multi-slice localizing images were acquired to check the animal's positioning in the magnet (repetition time = 100 ms, echo time (TE) = 2.8 ms, number of slices = 10, slice thickness = 1 mm).

Next, coronal and sagittal rapid acquisition with relaxation enhancement T_2-weighted images were acquired (repetition time = 4,000 ms, TE = 18 ms, echo train length = 8; averages = 2; field of view = $2.56 \times 2.56\,cm^2$; resolution = 256×256 pixels; number of slices = 20; slice thickness = 1 mm) and used to position the two ^{1}H-MRS voxels.

The first ^{1}H-MRS voxel was $2.7 \times 1.3 \times 2.7\,mm^3$ in the contused cortex immediately under the TBI impact (the 'cortical voxel'). The second was a $3 \times 2.5 \times 3\,mm^3$ voxel in normal-appearing tissue adjacent to the contusion site, which included the hippocampus, corpus callosum, and dorsal-most thalamic nuclei, primarily lateroposterior and laterodorsal (the 'hippocampal voxel'). Voxel positioning was based on anatomic landmarks, and care was taken to ensure reproducibility of the voxel position across scanning days. The average elapsed time from the TBI to the start of the first ^{1}H-MRS scan was <1 hour (58 ± 23 minutes).

We used a custom-made quadrature dual-coil transmit-receiver surface coil (each coil was 18 mm in diameter; Tkac *et al*, 1999). The ^{1}H-MRS was performed using a water-suppressed STEAM sequence (TE = 2 ms, repetition time = 4,000 ms; Tkac *et al*, 1999). First- and second-order shims were adjusted using FASTMAP (Gruetter, 1993) to achieve water line widths of 10 to 12 Hz before injury and 10 to 20 Hz after injury. Shimming was often more challenging in the focally injured environment of the cortex, likely due to local field inhomogeneities. If repeated shimming attempts could not achieve a line width of <20 Hz, then spectra were not collected.

Data were acquired as a series of free induction decays (each of which averaged 16 transients), corrected for frequency drift, averaged and corrected for eddy current effects. In the hippocampal voxel, we averaged 320 transients over a period of $\sim$21 minutes. In the smaller cortical voxel, we averaged 640 transients over $\sim$42 minutes. Spectra were analyzed with LCModel in the frequency domain (Provencher, 1993). LCModel uses a basis set of spectra acquired from *in vitro* samples of pure chemicals to estimate the *in vivo* neurochemical concentrations, and the unsuppressed water signal from the prescribed voxel as a reference for each scan to correct for small variations in coil sensitivity (Pfeuffer *et al*, 1999). Peak assignments for individual metabolites in the neurochemical profile were based on validated reports (Pfeuffer *et al*, 1999; Tkac *et al*, 2003). Neurochemical abbreviations are as follows: Ala = alanine, Asc = ascorbate, Asp = aspartate, Cr = creatine, GABA = gamma aminobutyric acid, Glc = glucose, Gln = glutamine, Glu = glutamate, GPC = glycerophosphocholine, GSH = glutathione, Ins = *myo*-inositol, Lac = lactate, MM = macromolecules, NAA = N-acetylaspartate, NAAG = N-acetylaspartatyl glutamate, PCho = phosphocholine, PCr = phosphocreatine, PE = phosphoethanolamine, Ser = serine, Tau = taurine, tCr = Cr + PCr, tCho = GPC + PCho, Glx = Glu + Gln.

Behavioral Assessment

The rotarod and beam walk tests were used to assess sensorimotor performance after CCI. Animals were trained on both tests for 5 days to establish a reliable baseline performance before injury. After CCI, behavioral testing was performed on D1, D3, D7, D10, and D14. On days when both behavioral assessment and imaging were planned, behavior was tested first to avoid anesthesia effects. Behavioral scores after injury were expressed as a percent of preinjury scores so that each animal served as its own control.

Rotarod: Rotarod training and testing were performed on a four-lane rotarod apparatus (Accuscan Instruments, Mentor, OH, USA) programmed with an accelerating task (0 to 30 rpm in 300 seconds). On each day, the latency to fall was recorded in three separate trials. Since distractions could influence rotarod performance, we used the maximum latency of the three trials as the score for each testing day, rather than the mean, as a reflection of the animal's capacity for motor function (Buitrago *et al*, 2004).

Beam walk: Beam walk training and testing followed a protocol adapted from Pleasant *et al* (2011). The testing was conducted on a custom-made 1 m long horizontal beam supported at a height of 50 cm. On each day, beam walk testing was performed with one trial each on beams of increasing difficulty (5 cm, 3.5 cm, 1.9 cm flat plank, and 2.5 cm rod). The beam walk was scored on a 0- to 12-point scale, with each trial assigned a score of 0 to 3 points: 3 points = crosses, no faults; 2 points = mildly impaired, crosses with 1 to 4 faults (paw slips off and falls below the plane of the beam); 1 point = moderately impaired, crosses with $\geqslant$5 faults, or falls upside down on the beam 1 to 3 times; 0 points = severely impaired; falls upside down on the beam $\geqslant$4 times, falls off the beam, or is unable to cross (maximum trial time = 120 seconds).

Reproducibility

To characterize the reproducibility of repeated ^{1}H-MRS measurements acquired in the same subjects over time, a separate group of uninjured age- and sex-matched rats ($n = 6$) was scanned in two sessions, 7 days apart. We used identical imaging protocols to those used in the TBI study for hippocampal ^{1}H-MRS. We compared means and coefficients of variation across sessions for four neurochemicals (NAA, Tau, Gln, and GSH) to represent a broad range of physiological concentrations and fitting reliabilities.

Statistical Analysis

The effect of TBI on behavioral test scores and neurochemical measures was evaluated with the mixed-effects model assuming a first-order autoregressive correlation structure. *Post hoc* comparisons between time points were evaluated based on the least-square means.

We set an initial acceptance threshold of $\leqslant$30% for the Cramér-Rao lower bounds of LCModel for each neurochemical fit. For some neurochemicals on some

days, concentration values decreased below the detection limits of our system resulting in Cramér-Rao lower bounds >30% even though the overall spectral quality was within our *a priori* acceptance criteria (line width <20 Hz, signal-to-noise ratio >8). Studies in our laboratory have shown that fitting reliability is dependent on spectral resolution and signal-to-noise ratio (unpublished results). Since excluding the measures with Cramér-Rao lower bounds >30% could cause overestimation of mean concentrations, we treated these measures as missing values and handled them by multiple imputations. This approach was based on the assumption that the unknown concentration values fall somewhere between the lower detection limit of our system and zero. We first estimated the detection limit for each neurochemical by identifying the minimum concentration detected with Cramér-Rao lower bounds ⩽30% (across all samples). Then, for each missing value, we performed multiple imputations (10 times) over a uniform distribution between the detection limit and zero. The TBI effect on each neurochemical was evaluated by the mixed-effects model after incorporating the imputed values. The results from the 10 imputations were combined to obtain the within- and between-imputation variance for making inference as in Schafer (Lubin *et al*, 2004; Schafer, 1997). Given multiple comparisons from 20 neurochemicals, the Benjamini-Yekutieli's procedure was applied to control the false discovery rate at 0.05.

Results

Functional Deficits after Sensorimotor Controlled Cortical Impact

The rotarod and beam walk tests confirmed that CCI to the sensorimotor cortex produced substantial motor deficits (Figure 1). The largest rotarod deficit was seen on D1 after TBI ($-56 \pm 19\%$, $P<0.0001$). Rotarod performance improved from D1 to D7 ($P=0.0009$) but not subsequently. On D14, rotarod performance remained significantly impaired compared with preinjury baseline ($-36 \pm 5\%$, $P<0.0001$). The largest beam walk deficit was also seen on D1 ($-52 \pm 12\%$, $P<0.0001$). Beam walk scores improved from D1 through D10 ($P<0.0001$) but not subsequently. On D14, beam walk performance remained significantly impaired compared with preinjury baseline ($-14 \pm 7\%$, $P=0.002$).

Lesion Characteristics on T_2-Weighted Magnetic Resonance Imaging

T_2-weighted MRI verified the tissue effects of CCI and allowed us to follow the longitudinal development of the brain contusion *in vivo* (Figure 2). Tissue disruption was visible on D0 (~1 hour after TBI), including cortical surface deformation, ventral shift of the corpus callosum, and frequent small intraparenchymal hemorrhages. On D1 to D3, edema could be seen as a diffuse hyperintensity in the ipsilateral cortex, and tissue swelling was indicated by displacement of the cortical surface and a midline shift toward the contralateral hemisphere. Tissue swelling had subsided by D7, giving way to cortical thinning and ventricular enlargement. On D14, a cortical cavity with discrete boundaries was visible, filled with hyperintense cerebrospinal fluid and hypointense blood products. The cortical cavity frequently appeared to connect with the enlarged ipsilateral ventricle.

Quality and Reproducibility of Proton Magnetic Resonance Spectra

High quality spectra with narrow line widths were generally obtained throughout the study. Before injury, mean line widths for the unsuppressed water resonance were 11.6 ± 0.6 Hz in the hippocampal voxel and 12.1 ± 1.0 Hz in the cortical voxel. After TBI, at the earliest time point (D0) mean line widths increased to 14.9 ± 1.6 Hz in the hippocampus and to 17.1 ± 2.3 Hz in the cortex, presumably due to acute tissue swelling and microhemorrhage. Line widths at all subsequent time points were similar to preinjury levels (D1 to D14 mean 12.6 ± 1.2 Hz in hippocampus; 12.1 ± 2.5 Hz in cortex).

Neurochemical concentrations measured with ^{1}H-MRS in the absence of TBI were highly reproducible. At two time points 7 days apart, mean NAA concentrations were 9.48 ± 0.50 and 9.25 ± 0.28 μmol/g, Gln was 2.78 ± 0.24 and 2.69 ± 0.23 μmol/g, Tau was

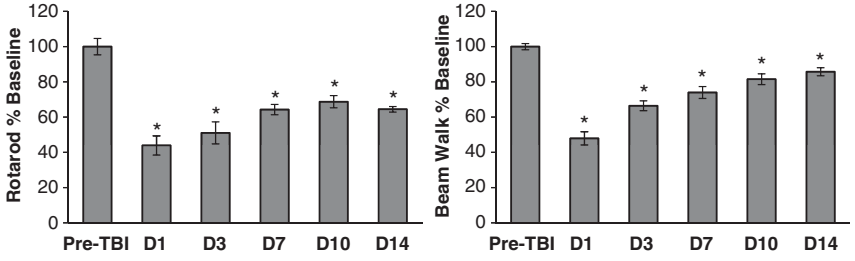

Figure 1 Motor behavioral deficits after controlled cortical impact (CCI) of the sensorimotor cortex. Postinjury scores on the rotarod and the beam walk were expressed as a percent of preinjury baseline scores for each animal. After traumatic brain injury (TBI), performance on both tasks was significantly impaired from D1 through D14 (*indicates $P < 0.05$ versus preTBI). Data are expressed as group mean ± standard error.

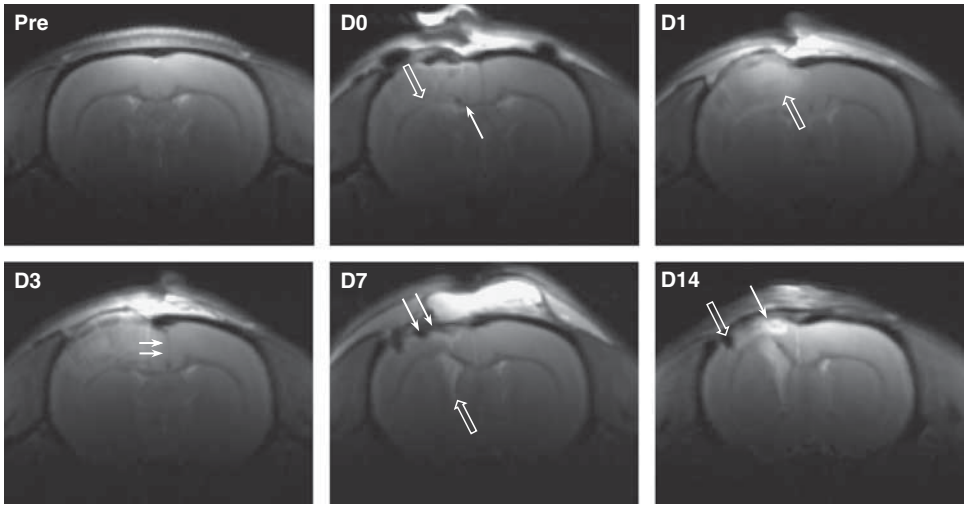

Figure 2 T_2-weighted magnetic resonance imaging (MRI) of a rat brain after controlled cortical impact (CCI). Representative coronal images (bregma −0.5 mm) show the development of the cortical contusion from Day 0 (D0, 1 hour after injury) to Day 14 (D14). Tissue disruption was visible early after injury, with ventral shift of the corpus callosum (open arrow, D0) and frequent small intraparenchymal hemorrhages (line arrow, D0). On D1 and D3, ipsilateral cortical edema was visible as a diffuse tissue hyperintensity (open arrow, D1), and brain swelling was indicated by a midline shift (line arrows, D3). By D7 the swelling had subsided, giving way to ipsilateral cortical thinning (line arrows, D7) and ventricular enlargement (open arrow, D7). By D14 a cortical contusion cyst had developed, filled with hyperintense cerebrospinal fluid (line arrow, D14) and/or hypointense blood products (open arrow, D14).

6.28 ± 0.15 and $6.25 \pm 0.16\,\mu$mol/g, and GSH was 0.91 ± 0.08 and $0.92 \pm 0.12\,\mu$mol/g, respectively. Neurochemical concentrations were not significantly different between time points (all P values >0.5, paired t-test). Although coefficients of variation varied across neurochemicals (2% to 13%), they were similar for each metabolite over time.

The Neurochemical Profile of Traumatic Brain Injury in Contused and Normal-Appearing Brain Regions

We used longitudinal *in vivo* ^{1}H-MRS to evaluate the postinjury evolution of 20 individual neurochemicals after TBI in two brain regions (Tables 1A and 1B). The cortical voxel for MRS was positioned directly under the impact and contained tissue that would degenerate into a visible contusion cavity. In the cortex, TBI led to significant changes in 19 out of 20 neurochemicals measured. Figure 3A presents a series of cortical spectra after TBI, showing dramatically altered spectral profiles.

N-acetylaspartate decreased rapidly after injury (−45% on D0), reached its lowest level on D3 (−83%), and remained significantly reduced through D14 (Figure 4; Table 1A). Ins and Tau were also reduced after TBI (Ins, −73% at D3; Tau, −61% at D3) but recovered toward baseline levels after D3. Ins continued to increase from D3 to D14 and was significantly elevated compared with baseline by D14 (+27%; Figure 4; Table 1A).

GPC and PCho showed differential changes after TBI (Figure 5; Table 1A). GPC decreased sharply by 1 hour after injury to levels below the detection limit of our system but had recovered to baseline by D7. By contrast, PCho was increased (∼270% to 450%) from D1 to D7 followed by a return to baseline by D14.

Neurotransmitters also showed differential changes. Although Glu was decreased in the cortex at all postinjury time points, Gln was increased at D0 (+205%) and D1 (+182%) before returning to baseline levels (Figure 5; Table 1A). Other neurotransmitters were also decreased in the contused cortical voxel, including GABA (maximum change of −46% on D1), NAAG (maximum change of −68% on D7), and Asp (maximum change of −81% on D0).

We observed sharp decreases in the antioxidants GSH and Asc in the injured cortex (Figure 4; Table 1A). GSH decreased on D0 to D3 to levels below the detection limit of our system and recovered to baseline levels by D7. Asc reached its lowest level at D3 (−69%) and remained significantly depleted through D14 (−44%).

Dramatic increases in Lac at the cortical injury site were seen by D0 (Figure 3A). Lac increased by ∼600% on D0 to D3 after injury, before falling back toward baseline values (Figure 4; Table 1A). Ala and Ser were also increased over a similar time course. Ala increases ranged from ∼350% to 550% on D0 to D3 before falling back to low baseline levels. Significant increases in Ser (120% to 200%) were seen between D0 and D14. By contrast, cortical Glc levels decreased from D0 to D3, reaching their lowest level on D3 (−50%) before recovering.

In summary, we observed substantial neurometabolic changes at the cortical contusion site, with 14 neurochemicals significantly decreased and 5 (Gln, PCho, Lac, Ala, and Ser) increased after TBI.

Table 1A Rat cortex: time course of neurochemical changes after TBI

	Pre	*D0*	*D1*	*D3*	*D7*	*D14*
Ala	0.25 ± 0.23^{i}	1.62 ± 0.31***	1.25 ± 0.24**	1.12 ± 0.22*	0.30 ± 0.33^{i}	0.30 ± 0.33^{i}
Asc	3.05 ± 0.20	1.41 ± 0.29***	1.34 ± 0.22***	0.94 ± 0.21***, ^{i}	1.64 ± 0.31**	1.70 ± 0.29**
Asp	2.43 ± 0.14	0.47 ± 0.24***, ^{i}	0.55 ± 0.17***, ^{i}	0.82 ± 0.16***, ^{i}	2.10 ± 0.21	1.1 ± 0.22***
Cr	3.65 ± 0.28	2.22 ± 0.40**	1.98 ± 0.29***	1.31 ± 0.28***	1.36 ± 0.40***	2.85 ± 0.39
GABA	0.89 ± 0.10	1.17 ± 0.14	0.48 ± 0.11*, ^{i}	0.55 ± 0.11*, ^{i}	1.13 ± 0.13	0.87 ± 0.14
Glc	3.17 ± 0.28	2.15 ± 0.39*	2.11 ± 0.29*	1.58 ± 0.28***	2.54 ± 0.39	2.6 ± 0.39
Gln	2.81 ± 0.35	5.77 ± 0.49***	5.11 ± 0.37***	2.96 ± 0.36	3.96 ± 0.50	3.15 ± 0.50
Glu	10.52 ± 0.39	6.27 ± 0.52***	5.14 ± 0.40***	3.72 ± 0.39***	5.62 ± 0.53***	5.43 ± 0.55***
GPC	0.62 ± 0.06	0.15 ± 0.09**, ^{i}	0.15 ± 0.07***, ^{i}	0.25 ± 0.06***, ^{i}	0.62 ± 0.08	0.83 ± 0.09
GSH	0.78 ± 0.09	0.29 ± 0.14*, ^{i}	0.28 ± 0.10**, ^{i}	0.28 ± 0.10**, ^{i}	0.82 ± 0.13	0.57 ± 0.13
Ins	5.52 ± 0.34	5.36 ± 0.47	2.28 ± 0.36***	1.47 ± 0.35***, ^{i}	5.98 ± 0.47	7.01 ± 0.48*
Lac	1.06 ± 0.62	7.72 ± 0.79***	6.87 ± 0.65***	7.66 ± 0.62***	2.07 ± 0.82	0.33 ± 0.88^{i}
MM	1.87 ± 0.07	1.46 ± 0.08***	1.16 ± 0.07***	0.85 ± 0.07***	0.45 ± 0.11***	0.48 ± 0.10***
NAA	9.83 ± 0.36	5.36 ± 0.42***	3.26 ± 0.37***	1.69 ± 0.36***	3.27 ± 0.44***	3.81 ± 0.49***
NAAG	0.97 ± 0.06	0.43 ± 0.10***	0.34 ± 0.08***, ^{i}	0.33 ± 0.07***, ^{i}	0.31 ± 0.11***, ^{i}	0.50 ± 0.10**
PCho	0.13 ± 0.06^{i}	0.16 ± 0.08^{i}	0.35 ± 0.06*	0.56 ± 0.06***	0.59 ± 0.08***	0.26 ± 0.08
PCr	4.90 ± 0.47	3.13 ± 0.60**	2.58 ± 0.49***	1.74 ± 0.47***	4.13 ± 0.62	2.53 ± 0.66**
PE	1.14 ± 0.25	1.84 ± 0.35	0.71 ± 0.26^{i}	0.86 ± 0.25^{i}	1.14 ± 0.35	0.39 ± 0.37^{i}
Ser	1.24 ± 0.40^{i}	3.81 ± 0.54***	2.76 ± 0.40*	1.73 ± 0.39	1.76 ± 0.55	2.96 ± 0.55
Tau	5.28 ± 0.32	3.74 ± 0.41**	2.96 ± 0.33***	2.05 ± 0.32***	4.43 ± 0.42	4.20 ± 0.45
tCr (Cr+PCr)	8.55 ± 0.38	6.82 ± 0.46**	4.61 ± 0.39***	3.03 ± 0.38***	6.05 ± 0.48**	5.44 ± 0.42***
tCho (GPC+PCho)	0.82 ± 0.06	0.29 ± 0.08***	0.53 ± 0.06**	0.78 ± 0.06	1.29 ± 0.08***	1.20 ± 0.08***
Glx (Glu+Gln)	13.33 ± 0.68	11.94 ± 0.91	10.30 ± 0.71**	6.63 ± 0.68***	9.50 ± 0.93**	8.54 ± 0.96**

Ala, alanine; Asp, aspartate; Asc, ascorbate; Cr, creatine; GABA, gamma aminobutyric acid; Glc, glucose; Gln, glutamine; Glu, glutamate; GPC, glycerophosphocholine; GSH, glutathione; Ins, *myo*-inositol; Lac, lactate; MM, macromolecules; NAA, N-acetylaspartate; NAAG, N-acetylaspartatyl glutamate; PCho, phosphocholine; PCr, phosphocreatine; PE, phosphoethanolamine; Ser, serine; Tau, taurine; tCho, total choline; tCr, total creatine; TBI, traumatic brain injury.
Concentrations are expressed as μmol/g wet tissue weight. Compared with preinjury values *indicates $P < 0.05$, **$P < 0.005$, ***$P < 0.0001$. *i* indicates groups with four or more values imputed.

Table 1B Rat hippocampus: time course of neurochemical changes after TBI

	Pre	*D0*	*D1*	*D3*	*D7*	*D14*
Ala	0.44 ± 0.04	0.56 ± 0.04	0.45 ± 0.04	0.42 ± 0.04	0.34 ± 0.05	0.35 ± 0.05
Asc	2.83 ± 0.11	2.45 ± 0.11	2.79 ± 0.11	2.82 ± 0.11	2.64 ± 0.11	2.68 ± 0.12
Asp	1.97 ± 0.12	1.38 ± 0.13**	1.66 ± 0.12	1.97 ± 0.12	2.02 ± 0.12	1.69 ± 0.14
Cr	3.93 ± 0.10	3.53 ± 0.10**	3.34 ± 0.10***	3.43 ± 0.10**	3.54 ± 0.10*	3.32 ± 0.11***
GABA	1.37 ± 0.05	1.42 ± 0.05	1.36 ± 0.05	1.35 ± 0.05	1.40 ± 0.05	1.36 ± 0.06
Glc	1.87 ± 0.20	1.48 ± 0.22^{i}	1.68 ± 0.21	1.64 ± 0.20	2.06 ± 0.21	2.12 ± 0.23
Gln	2.61 ± 0.08	2.81 ± 0.09*	3.05 ± 0.09**	3.64 ± 0.08***	2.79 ± 0.09	2.62 ± 0.10
Glu	10.20 ± 0.19	8.42 ± 0.19***	9.79 ± 0.19	9.32 ± 0.19**	9.82 ± 0.19	9.37 ± 0.21*
GPC	0.85 ± 0.04	0.65 ± 0.04***	0.88 ± 0.04	0.79 ± 0.04	0.83 ± 0.04	0.78 ± 0.04
GSH	0.92 ± 0.03	0.87 ± 0.04	0.75 ± 0.04	0.78 ± 0.03	0.82 ± 0.04	0.79 ± 0.04
Ins	7.37 ± 0.15	6.88 ± 0.16**	6.64 ± 0.16**	6.75 ± 0.15**	7.55 ± 0.16	7.55 ± 0.17
Lac	1.74 ± 0.14	1.91 ± 0.14	2.14 ± 0.14*	1.81 ± 0.14	1.49 ± 0.14	1.31 ± 0.16*
MM	2.03 ± 0.03	1.76 ± 0.03***	1.75 ± 0.03***	1.76 ± 0.03***	1.89 ± 0.03**	1.82 ± 0.04***
NAA	9.30 ± 0.17	8.24 ± 0.17***	8.29 ± 0.17***	8.05 ± 0.17***	8.66 ± 0.17*	8.69 ± 0.19*
NAAG	0.90 ± 0.03	0.96 ± 0.03	0.99 ± 0.03	1.00 ± 0.03	1.05 ± 0.03	0.99 ± 0.04
PCho	0.23 ± 0.05^{i}	0.27 ± 0.04^{i}	0.20 ± 0.05^{i}	0.40 ± 0.04	0.34 ± 0.04	0.30 ± 0.05
PCr	5.57 ± 0.13	5.13 ± 0.14	5.56 ± 0.14	5.54 ± 0.13	5.45 ± 0.14	5.16 ± 0.15
PE	1.76 ± 0.15	1.44 ± 0.16^{i}	1.47 ± 0.15	1.46 ± 0.15	1.84 ± 0.15	1.67 ± 0.17
Ser	0.81 ± 0.18^{i}	1.55 ± 0.19^{i}	1.02 ± 0.19	1.11 ± 0.18	0.86 ± 0.19^{i}	0.88 ± 0.21^{i}
Tau	6.38 ± 0.14	5.77 ± 0.14	5.88 ± 0.14	6.01 ± 0.14	6.07 ± 0.14	5.96 ± 0.16
tCr (Cr+PCr)	9.50 ± 0.15	8.66 ± 0.15***	8.91 ± 0.15**	8.97 ± 0.15*	8.98 ± 0.15*	8.49 ± 0.17***
tCho (GPC+PCho)	1.12 ± 0.04	0.98 ± 0.05*	1.12 ± 0.05	1.20 ± 0.04	1.18 ± 0.05	1.10 ± 0.05
Glx (Glu+Gln)	12.81 ± 0.24	11.24 ± 0.25***	12.84 ± 0.25	12.96 ± 0.24	12.60 ± 0.25	11.99 ± 0.28*

Ala, alanine; Asp, aspartate; Asc, ascorbate; Cr, creatine; GABA, gamma aminobutyric acid; Glc, glucose; Gln, glutamine; Glu, glutamate; GPC, glycerophosphocholine; GSH, glutathione; Ins, *myo*-inositol; Lac, lactate; MM, macromolecules; NAA, N-acetylaspartate; NAAG, N-acetylaspartatyl glutamate; PCho, phosphocholine; PCr, phosphocreatine; PE, phosphoethanolamine; Ser, serine; Tau, taurine; tCho, total choline; tCr, total creatine; TBI, traumatic brain injury.
Concentrations are expressed as μmol/g wet tissue weight. Compared with preinjury values *indicates $P < 0.05$, **$P < 0.005$, ***$P < 0.0001$. *i* indicates groups with four or more values imputed.

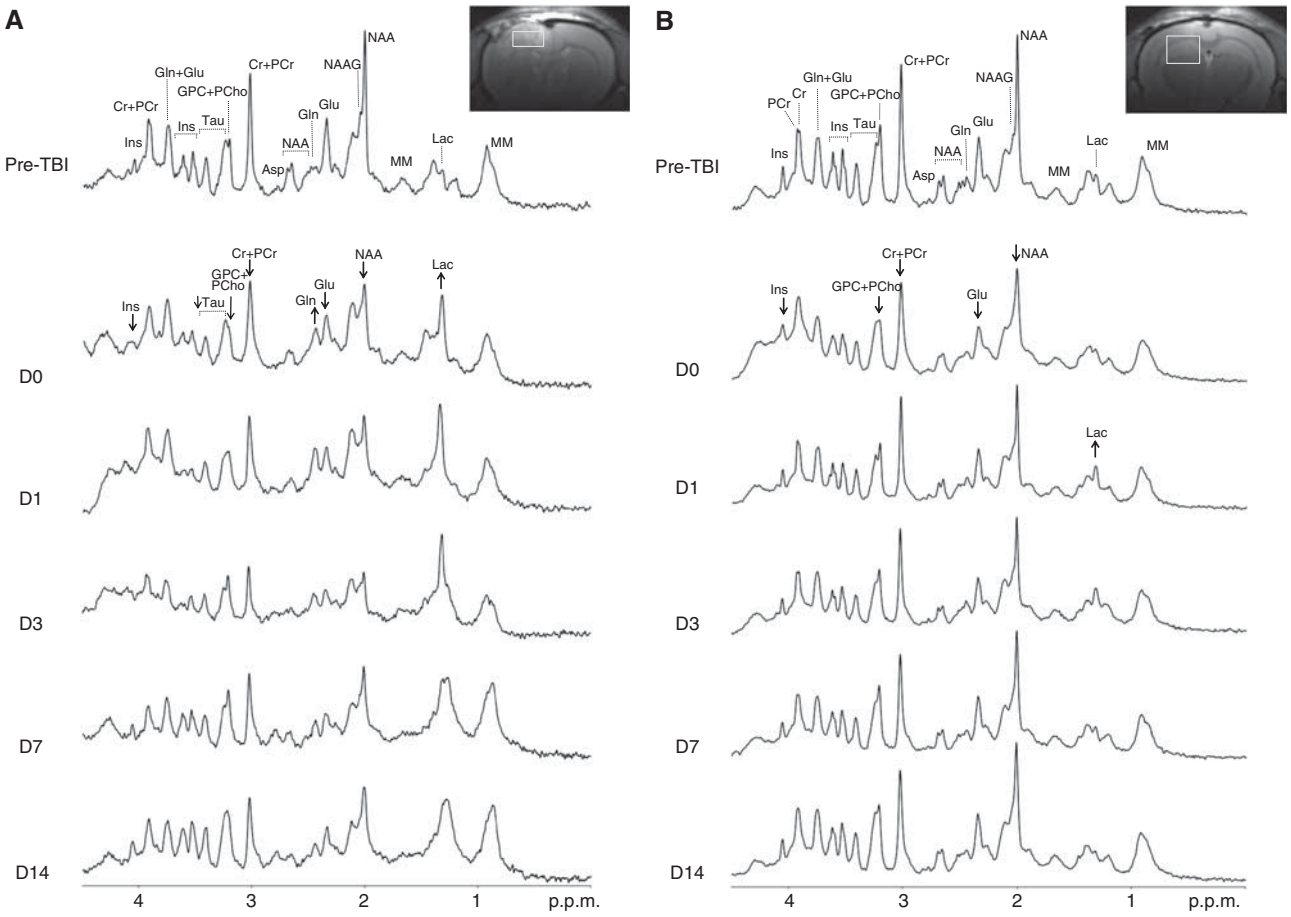

Figure 3 Representative proton magnetic resonance spectroscopy (^{1}H-MRS) spectra acquired before and after traumatic brain injury (TBI) in cortex and hippocampus. (**A**) A T_2-weighted coronal image from D3 shows the location of the cortical voxel at the site of the developing cerebral contusion. In the series of cortical spectra, neurochemical changes are apparent as early as D0 (1 hour after TBI). These include increased Lac and Gln, and decreased NAA, Glu, Cr + PCr, GPC + PCho, Tau, and Ins. NAA and Cr + PCr continue to decrease over time, reaching their lowest levels by D3. On D14, the cortical spectrum remains significantly altered compared with preinjury baseline. (**B**) A T_2-weighted coronal image from D3 shows the location of the hippocampal voxel, caudal to the cortical contusion in normal-appearing tissue. Despite the anatomically normal appearance of this voxel, the series of MR spectra show significant neurochemical changes after TBI. At D0, NAA, Glu, Cr + PCr, GPC + PCho, and Ins are visibly decreased, and by D1 Lac is visibly increased. Asp, aspartate; Cr, creatine; Glc, glucose; Gln, glutamine; Glu, glutamate; GPC, glycerophosphocholine; Ins, *myo*-inositol; Lac, lactate; MM, macromolecules; NAA, N-acetylaspartate; NAAG, N-acetylaspartatyl glutamate; PCho, phosphocholine; PCr, phosphocreatine; Tau, taurine.

The hippocampal voxel was positioned ipsilateral to TBI but farther from the impact site. Despite the lack of visible contusion in this location (Figure 3B), ^{1}H-MRS revealed significant changes in nine neurochemicals after TBI. NAA decreased early after TBI (−12% at D0) and remained significantly decreased compared with preinjury through D14 (Figure 4; Table 1B). Ins was decreased on D0 to D3 (−7% to −10%) but returned to control levels by D7 (Figure 4; Table 1B). Similar to our findings in the cortex, Glu was decreased (maximum change of −17% on D0) and Gln was increased (maximum change of +39% on D3) after TBI. Both Asp (−30%) and GPC (−24%) were transiently decreased at D0, returning to baseline levels by D1. By contrast, a postinjury decrease in Cr was sustained from D0 (−10%) until D14 (−15%). Hippocampal Lac was increased after TBI (maximum change of +23% on D1; Figure 4 and Table 1B).

Although the hippocampal patterns of change for an additional eight neurochemicals (Ala, Asc, PCho, PCr, GSH, NAAG, Ser, and Tau) were generally similar to those in the cortex, they were of lower magnitude and did not survive rigorous statistical correction for multiple comparisons (Table 1B). The plots in Figure 4 illustrate the regional difference in severity of neurochemical changes after TBI.

Discussion

This study has characterized the neurometabolic effects of TBI using high field ^{1}H-MRS to resolve

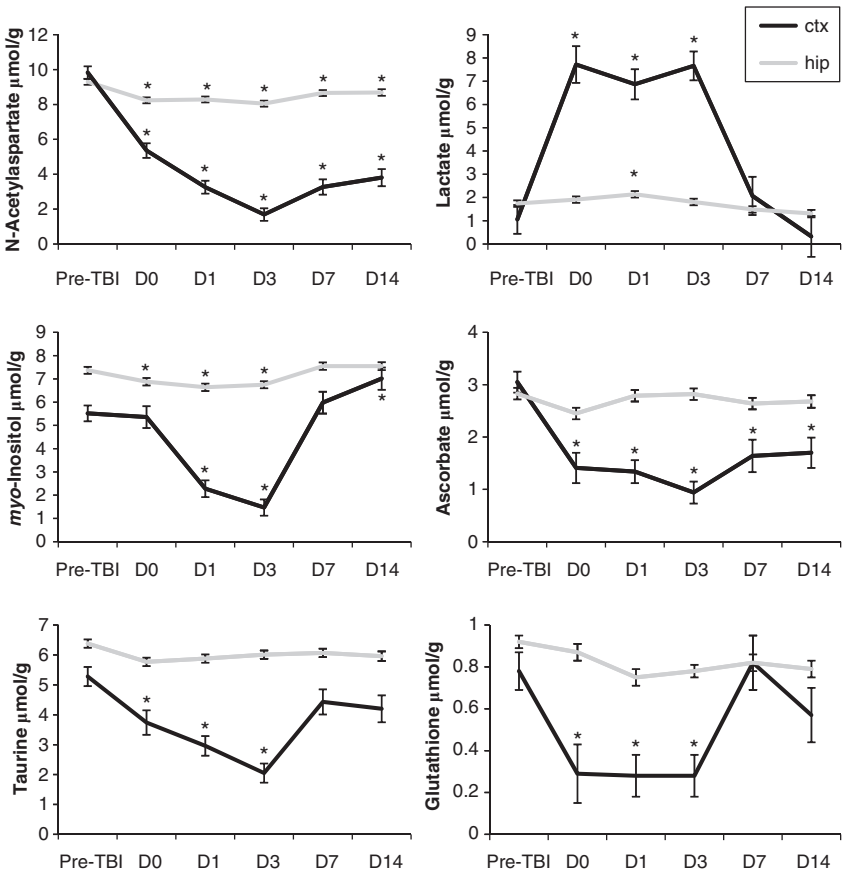

Figure 4 Changes in selected neurochemicals measured with proton magnetic resonance spectroscopy (^{1}H-MRS) after traumatic brain injury (TBI) (*indicates $P < 0.05$ versus preTBI). Data are expressed as mean ± standard error. ctx, cortical voxel, hip, hippocampal voxel.

20 metabolites in the rat brain *in vivo*. We examined the neurochemical changes in response to TBI in the cortex and hippocampus over a comprehensive time course from 1 hour to 2 weeks after injury. The cortical voxel, located directly under the cortical impact, contained focally injured tissue that degenerated into a visible contusion cavity. The more distal hippocampal voxel appeared undisturbed on T_2-weighted MRI throughout the 14-day study. Together, our ^{1}H-MRS results from these two regions suggest that the neurochemical profile after brain trauma provides an *in vivo* measure of local injury severity. These findings build on the recent report of Lescot *et al* (2010) showing regional, severity-dependent changes in NAA, tCho, and Lac after fluid percussion injury.

Proton Magnetic Resonance Spectroscopy Metabolites as Specific Biomarkers of Traumatic Brain Injury Pathology

The neurochemical profile detected by ^{1}H-MRS provides a snapshot of the *in vivo* metabolic status of cells in the brain. Changes in individual neurochemicals after TBI have been proposed to reflect specific cellular mechanisms of injury. Thus, the full neurochemical profile provides potential biomarkers representing several aspects of TBI pathology. Compared with biomarkers measured in serum or cerebrospinal fluid, neurochemical biomarkers measured with ^{1}H-MRS have the advantage of being directly assessed in the tissue of interest, and are likely to provide improved temporal and spatial precision. Since MRS measures include the intracellular space, this approach provides complementary information to that provided by microdialysis probes. Nonetheless, the links between specific neurochemicals and TBI mechanisms remain somewhat speculative. Furthermore, changes in certain of these neurochemicals might reflect the contributions of multiple, perhaps interacting, pathological mechanisms. Additional studies to elucidate the biological significance of these biomarkers are clearly warranted. In the following, we describe how changes to the neurochemical profile seen in our study might be associated with specific aspects of TBI pathology (summarized in Table 2).

Edema: We found postinjury reductions in Tau, Ins, NAA, and Glu, each of which may have a role as a

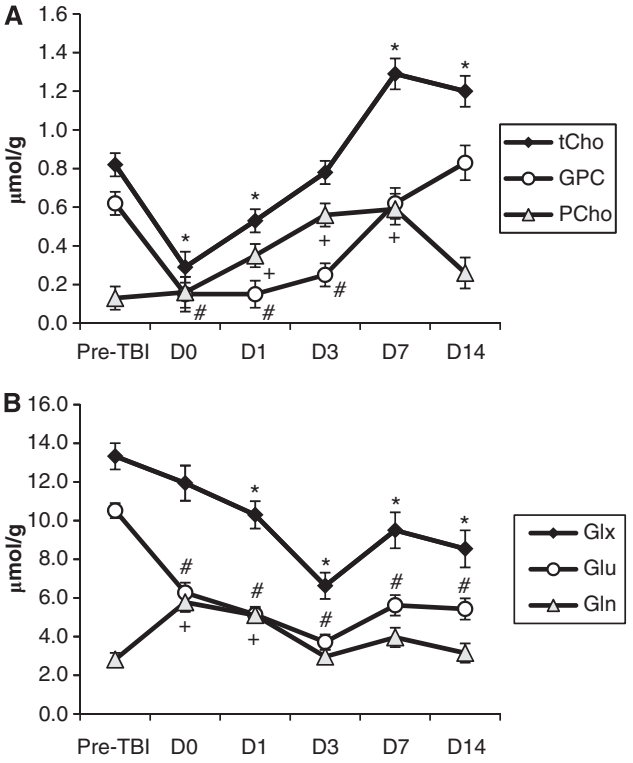

Figure 5 Increased spectral resolution at high field strength permits independent measurement of choline-containing compounds, glutamate, and glutamine. (**A**) Changes in choline-containing compounds in the contused cortex after traumatic brain injury (TBI). Compared with preinjury levels, tCho was decreased on D0 and D1 but elevated on D7 and D14 (* indicates $P < 0.05$). We resolved the individual changes in GPC and PCho after TBI, showing a decrease in GPC on D0 to D3 versus preinjury (# indicates $P < 0.05$) and an increase in PCho on D1 to D7 versus preinjury (+ indicates $P < 0.05$). (**B**) Changes in Glx, Glu, and Gln in the contused cortex after TBI. Compared with preinjury levels, Glx was significantly lower on D1 to D14 (* indicates $P < 0.05$). We resolved the individual changes in Glu and Gln after TBI, showing a decrease in Glu lasting from D0 to D14 (# indicates $P < 0.05$) and an increase in Gln on D0 and D1 (+ indicates $P < 0.05$). Data are expressed as mean ± standard error. tCho, total choline (GPC + PCho); GPC, glycerophospocholine; PCho, phosphocholine; Glx, (Glu + Gln); Glu, glutamate; Gln, glutamine.

cellular osmolyte. After TBI, blood–brain barrier disruption allows water to move from the vascular to the extracellular compartment (vasogenic edema) followed by cellular uptake (cytotoxic edema). To maintain volume homeostasis, brain cells exude organic osmolytes including Tau, Ins, NAA, and Glu (Moffett *et al*, 2006). Previous MRS studies have suggested that decreases in Tau and Ins may be associated with brain edema (Xu *et al*, 2011), and the lower NAA and Glu seen in this study might also be part of a homeostatic response to osmotic stress. Elevated brain water content after CCI has been documented over a similar time course to our observed reductions in Tau, Ins, NAA, and Glu (Markgraf *et al*, 2001).

Excitotoxicity and disrupted neurotransmission: Our observation of a decrease in Glu and an increase in Gln as early as 1 hour after CCI is consistent with Glu release from neurons followed by rapid uptake and conversion to Gln by astrocytes (Bartnik *et al*, 2005). Decreased Glu concomitant with increased Gln has also been reported after cerebral ischemia and mild TBI (Lei *et al*, 2009; Xu *et al*, 2011). Traumatic brain injury induces a rapid cascade of neuronal depolarization and release of the excitatory neurotransmitter glutamate. The resulting overstimulation of glutamate receptors initiates excitotoxic mechanisms culminating in neuronal damage. Thus, ^{1}H-MRS measurements of Glu and its metabolic derivative Gln may provide insight into excitotoxicity after TBI.

We also found postinjury decreases in cortical NAAG, Asp, and GABA, suggesting further disruption of neurotransmission. These results are supported by electrophysiological evidence of changes in the balance of neuronal excitation and inhibition as early as 1 day after injury (Imbrosci and Mittmann, 2011). We postulate that the decrease in NAAG and Asp may result from reduced availability of precursor NAA, while lower GABA may arise from reduced availability of precursor Glu. Altered activation of protein kinases after TBI may further contribute to NAAG suppression (Arun *et al*, 2006).

Neurotransmitter changes in the perilesional hippocampus were generally similar to those in the cortex although of lower magnitude, suggesting that postinjury disruption of neurotransmission extends beyond the immediate contusion. Our finding of slightly increased NAAG in the hippocampus clearly contrasted with the large decrease in NAAG at the cortical contusion. Since NAAG can promote the release of protective growth factors (Zhou *et al*, 2005), we speculate that increased NAAG might represent an endogenous neuroprotective response.

Oxidative stress: GSH and Asc, two endogenous antioxidants with the highest concentration in the central nervous system (Rice and Russo-Menna, 1998), function in concert to detoxify free radicals. We interpret the dramatic depletion of GSH and Asc we observed in the cortical voxel as an indicator of severe oxidative stress, consistent with previous findings from brain extracts after experimental TBI (Ansari *et al*, 2008; Tavazzi *et al*, 2005). The smaller antioxidant decrease we observed in the hippocampus suggests a milder disruption of cellular redox state in the perilesional zone. Given that GSH is found at higher concentrations in glia while Asc predominates in neurons (Rice and Russo-Menna, 1998), our results suggest that oxidative stress affects both major cell types after neurotrauma.

Neuronal and glial integrity: It is likely that the sustained reduction of NAA we report in the injured cortex reflects substantial focal neuronal loss after CCI (Chen *et al*, 2003). In contrast, the smaller sustained decrease in hippocampal NAA may

Table 2 ^{1}H-MRS neurochemicals and their relevance to TBI pathophysiology

Abbreviation	*Neurochemical*	*Putative role*
Ala	Alanine	Bioenergetics
Asc	Ascorbate	Oxidative stress
Asp	Aspartate	Excitatory neurotransmission; bioenergetics
Cr	Creatine	Bioenergetics
GABA	γ-aminobutyric acid	Inhibitory neurotransmission
Glc	Glucose	Bioenergetics
Gln	Glutamine	Excitatory neurotransmission
Glu	Glutamate	Excitatory neurotransmission; edema
GPC	Glycerophosphocholine	Membrane turnover
GSH	Glutathione	Oxidative stress
Ins	*myo*-Inositol	Edema; glial marker
Lac	Lactate	Hypoxia/ischemia; bioenergetics
MM	Macromolecules	Cellular mass/cytosolic proteins
NAA	N-acetylaspartate	Neuronal marker; edema; bioenergetics
NAAG	N-acetylaspartylglutamate	Inhibitory neurotransmission; neuroprotection
PCho	Phosphocholine	Membrane turnover; glial proliferation
PCr	Phosphocreatine	Bioenergetics
PE	Phosphoethanolamine	Free fatty acids
Ser	Serine	Bioenergetics
Tau	Taurine	Edema

TBI, traumatic brain injury; ^{1}H-MRS, proton magnetic resonance spectroscopy.

represent diffuse neurodegeneration remote from the cortical injury (Hall *et al*, 2008). N-acetylaspartate is primarily restricted to neurons, so prolonged decreases in NAA after TBI have been attributed to neurodegeneration or diffuse axonal injury (Moffett *et al*, 2006). Further evidence for NAA as a neuronal marker is provided by reports that NAA levels on ^{1}H-MRS correlate with histological measures of neuronal and axonal density (Brooks *et al*, 2010; Schuhmann *et al*, 2003). Moreover, in TBI survivors NAA levels correlate with injury severity and functional outcome (Garnett *et al*, 2000).

Since Ins is found at high concentrations in astrocytes, Ins measured with ^{1}H-MRS has been proposed to serve as a glial marker (Brand *et al*, 1993). In the present study, the initial Ins reduction after TBI could reflect astrocyte cell death, which has been reported as early as 30 minutes after experimental TBI (Zhao *et al*, 2003). The recovery of Ins after D3 may indicate reactive glial proliferation, consistent with a reported increase in GFAP immunostaining that paralleled increased levels of Ins after TBI (Schuhmann *et al*, 2003).

The decrease in MM we observed starting 1 hour after injury could be interpreted as a degradation of cellular structural integrity under pathogenic conditions (Lei *et al*, 2009), since the MM resonances of the proton magnetic resonance spectrum have been attributed to cytosolic proteins (Behar and Ogino, 1993). We speculate that the MM decrease may be related to increased activity of cytosolic proteases, including caspases and calpain, that has been observed within minutes to hours after TBI (Saatman *et al*, 2010).

Cell membrane turnover and inflammation: The mechanical strain sustained during TBI causes both immediate and delayed damage to neuronal and glial plasma membranes, releasing membrane phospholipids that are often reported as tCho. Increased tCho has been described in human TBI (Brooks *et al*, 2000) whereas lower tCho is seen in animal models, which typically probe earlier in the time course of injury (Schuhmann *et al*, 2003). Our current findings show that at 9.4 T, differential changes in GPC and PCho, the two main components of tCho, can be resolved. Moreover, they suggest that the observed early decrease in tCho might be explained by a dramatic decrease in GPC, whereas a subsequent elevation of tCho appears to result from recovery of GPC accompanied by elevated PCho. Since high PCho has also been attributed to cell proliferation in glial-derived tumors (Righi *et al*, 2009), our reported rise in PCho might additionally reflect the proliferation of reactive astroglia at the contusion site that has been documented on days 1 to 7 after CCI (Chen *et al*, 2003; Schuhmann *et al*, 2003).

Bioenergetics: Our finding of decreased NAA after TBI might reflect mitochondrial dysfunction, since synthesis of NAA in neuronal mitochondria is strictly related to energetic metabolism (Bates *et al*, 1996). N-acetylaspartate has been proposed as a biomarker of neuronal mitochondrial status (Moffett *et al*, 2006). Notably, treating rats with cyclosporine A, a drug that protects mitochondrial function, was shown to preserve NAA and ATP levels after TBI (Signoretti *et al*, 2004).

Our finding of increased Lac, Ser, and Ala after injury provides further evidence of mitochondrial impairment. Indeed, elevated levels of these compounds are used as clinical evidence of electron transport chain disorders. Elevated Lac seen in both animal models and human MRS studies is commonly taken as evidence of hypoxia or ischemia and is associated with poor patient outcomes after TBI (Ashwal *et al*, 2000). Our expanded neurochemical profile shows that other glycolytic by-products, Ser and Ala, are also elevated after TBI indicating anaerobic glycolysis, probably at the expense of oxidative phosphorylation. In particular, elevated Ser indicates interrupted metabolism of glycolytic 3-phosphoglycerate. Similarly, when pyruvate carbons are unable to enter the citric acid cycle, they are redirected to Ala and Lac (Xing *et al*, 2012).

Our observed decrease in Glc after TBI appeared to be slower than the rapid change of other neurochemicals associated with energy metabolism. The progressive lowering of Glc we measured over several days after TBI is consistent with observations in

human survivors of brain injury (Yokobori *et al*, 2011). Indeed, whether brain Glc levels should be controlled after TBI is the subject of some debate. The ^{1}H-MRS might provide valuable clinical information on brain Glc levels after trauma. However, interpretation of Glc changes presents additional challenges since our observation of lower Glc likely reflects the combined effects of increased metabolism, reduced supply of circulating Glc, and uptake deficits.

The lower Asp we observed might result from reduced availability of Glu, which is depleted rapidly from the neuron after TBI. Asp is synthesized in the mitochondrion from Glu and oxaloacetate in a transaminase reaction that also produces α-ketoglutarate for entry into the citric acid cycle. Although we did not measure α-ketoglutarate we speculate that its production would also be lower, resulting in compromised citric acid cycle energy production.

We found that brain tCr decreases dramatically in the contused cortex and more subtly in the hippocampus after CCI. Intracellular Cr and PCr provide diffusable energy intermediates that are critical to normal cellular bioenergetics and function. Although the total creatine pool (Cr + PCr, i.e., tCr) is often assumed to remain relatively constant under physiological conditions, leading to its use as a reference for ^{1}H-MRS studies, our results add to ample evidence that tCr may be unstable in the context of brain injury (Gasparovic *et al*, 2009; Schuhmann *et al*, 2003; Xu *et al*, 2011).

Resolution of 20 Neurochemicals with High Field Proton Magnetic Resonance Spectroscopy: Technical Considerations

Previous *in vivo* ^{1}H-MRS studies of TBI have been limited to relatively few compounds, primarily NAA, Glx, Ins, Lac, Tau, tCho, and tCr. In the present study, the increased resolution and sensitivity provided by 9.4 T, ultra-short TE, and efficient water suppression, provided a far more detailed neurochemical profile.

The benefit of increased spectral resolution is highlighted in Figure 5. At lower magnetic field strengths including those used in most studies in humans, GPC and PCho are not well resolved and are usually reported as a single resonance, total choline (tCho). As noted above, previous findings of altered tCho after TBI have been inconsistent. However, unambiguous quantification at high field strength suggests differential behavior of the individual components. Similarly, findings related to Glu and Gln are often reported as a single combined Glx resonance at lower field strengths. Our data clearly indicate that changes in Glx result from a dramatic and rapid decrease in Glu in the presence of an increase in Gln.

Despite the increased sensitivity of neurochemical measurements at higher field strengths, certain neurochemicals decreased below detection limits at some time points after TBI. Imputation is a validated approach to estimating such missing values that allowed us to complete the time course for 20 neurochemicals after TBI. Accordingly, we have characterized the temporal evolution of several compounds in the injured brain for the first time. These include membrane components PCho and GPC, the neutral amino acids Ala and Ser, endogenous antioxidants Asc and GSH, as well as other neurochemicals such as Asp, NAAG, MM, and Glc. Imputation was particularly helpful for compounds that changed dramatically after TBI. For example, GSH was reliably detected before injury, but decreased sharply in the cortex after injury to levels below the detection limit in some animals (Figure 4; Table 1A). Conversely, some neurochemicals, such as PCho, became detectable after injury (Figure 5; Table 1A).

Reproducibility of neurochemical measures in the absence of injury was very high. For all selected neurochemicals, the variability in the uninjured brain was small compared with the magnitude of changes after TBI. For example, hippocampal NAA decreased by up to 13% after TBI versus a detected 2% difference in the uninjured brain. Similarly, hippocampal Gln increased by 39% after TBI versus a 3% difference in the uninjured brain. Although we did not characterize reproducibility in the cortex, we anticipate a similar stability to that observed in the hippocampus.

Our approach of using the unsuppressed water signal from each voxel to correct for coil sensitivity, although commonly used for spectroscopic quantification, might be susceptible to alterations to the water reference signal from physiological sources, e.g., from edema, cerebrospinal fluid invasion, or hemorrhage. At the extremely short TE used (2 ms), T_2 effects from such changes would be very small. However, to further explore the possible contribution of water referencing on neurochemical quantification we compared line width and integral of the water signal from each voxel over time. Although the line widths increased at the 1-hour time point, perhaps due to hemorrhage associated with TBI, the water integral did not increase suggesting that edema did not have a substantial effect on metabolite quantification. Moreover, any edema effect on the water reference signal would affect all neurochemicals to a similar degree, and certainly would move their concentration in the same direction. Our observation that after injury some neurochemicals decrease in concentration while others increase provides further evidence that any effects of water referencing on quantification are small compared with actual changes in neurochemical concentration.

Translational Potential of Proton Magnetic Resonance Spectroscopy for Traumatic Brain Injury Patients

The rich information in the neurochemical profile provides *in vivo* insight into the mechanisms and evolution of TBI pathology that may be useful for facilitating translation of novel therapies. Several of the neurochemicals we have described cannot be

resolved at present on existing clinical scanners, even at 3 T. However, technological developments continue to expand the flexibility and utility of ^{1}H-MRS in humans; for example, more sophisticated sequences have recently become available to quantify GSH and Asc on clinical 3 T scanners (Choi *et al*, 2011). From a research perspective, human MRI systems up to 8 T are now producing high quality MRS results and will likely permit an expanded neurochemical profile in humans.

Survivors of TBI often have symptoms that cannot be explained by macroscopic lesions visible with conventional brain imaging techniques. Existing clinical ^{1}H-MRS studies have provided insight into the neurochemical status of the injured brain, and we anticipate that additional biomarkers will greatly enhance our ability to monitor injury pathology. Moreover, if detected early, metabolic changes could be useful for predicting the location and extent of ultimate tissue damage, and could help to optimize treatment strategies and define intervention windows.

In summary, the neurochemical profile obtained at high field strength can provide valuable insight into the complex, dynamic responses of the brain after injury. As the relationships between neurochemicals visible with ^{1}H-MRS and pathological mechanisms of TBI are further elucidated, we anticipate that ^{1}H-MRS will become increasingly valuable for assessing human survivors of TBI and developing novel therapies.

Acknowledgements

The content is solely the responsibility of the authors and does not necessarily represent the official views of the NIH.

Disclosure/conflict of interest

The authors declare no conflict of interest.

References

Ansari MA, Roberts KN, Scheff SW (2008) A time course of contusion-induced oxidative stress and synaptic proteins in cortex in a rat model of TBI. *J Neurotrauma* 25: 513–26

Arun P, Madhavarao CN, Moffett JR, Namboodiri MA (2006) Regulation of N-acetylaspartate and N-acetylaspartylglutamate biosynthesis by protein kinase activators. *J Neurochem* 98:2034–42

Ashwal S, Holshouser B, Tong K, Serna T, Osterdock R, Gross M, Kido D (2004) Proton spectroscopy detected myoinositol in children with traumatic brain injury. *Pediatr Res* 56:630–8

Ashwal S, Holshouser BA, Shu SK, Simmons PL, Perkin RM, Tomasi LG, Knierim DS, Sheridan C, Craig K, Andrews GH, Hinshaw DB (2000) Predictive value of proton magnetic resonance spectroscopy in pediatric closed head injury. *Pediatr Neurol* 23:114–25

Babikian T, Freier MC, Ashwal S, Riggs ML, Burley T, Holshouser BA (2006) MR spectroscopy: predicting long-term neuropsychological outcome following pediatric TBI. *J Magn Reson Imaging* 24:801–11

Bartnik BL, Sutton RL, Fukushima M, Harris NG, Hovda DA, Lee SM (2005) Upregulation of pentose phosphate pathway and preservation of tricarboxylic acid cycle flux after experimental brain injury. *J Neurotrauma* 22:1052–65

Bates TE, Strangward M, Keelan J, Davey GP, Munro PM, Clark JB (1996) Inhibition of N-acetylaspartate production: implications for 1H MRS studies *in vivo*. *Neuroreport* 7:1397–400

Behar KL, Ogino T (1993) Characterization of macromolecule resonances in the 1^{H} NMR spectrum of rat brain. *Magn Reson Med* 30:38–44

Brand A, Richter-Landsberg C, Leibfritz D (1993) Multinuclear NMR studies on the energy metabolism of glial and neuronal cells. *Dev Neurosci* 15:289–98

Brooks WM, Friedman SD, Gasparovic C (2001) Magnetic resonance spectroscopy in traumatic brain injury. *J Head Trauma Rehabil* 16:149–64

Brooks WM, Sibbitt Jr WL, Kornfeld M, Jung RE, Bankhurst AD, Roldan CA (2010) The histopathologic associates of neurometabolite abnormalities in fatal neuropsychiatric systemic lupus erythematosus. *Arthritis Rheum* 62: 2055–63

Brooks WM, Stidley CA, Petropoulos H, Jung RE, Weers DC, Friedman SD, Barlow MA, Sibbitt Jr WL, Yeo RA (2000) Metabolic and cognitive response to human traumatic brain injury: a quantitative proton magnetic resonance study. *J Neurotrauma* 17:629–40

Buitrago MM, Schulz JB, Dichgans J, Luft AR (2004) Short and long-term motor skill learning in an accelerated rotarod training paradigm. *Neurobiol Learn Mem* 81:211–6

Chen S, Pickard JD, Harris NG (2003) Time course of cellular pathology after controlled cortical impact injury. *Exp Neurol* 182:87–102

Choi IY, Lee SP, Denney DR, Lynch SG (2011) Lower levels of glutathione in the brains of secondary progressive multiple sclerosis patients measured by 1H magnetic resonance chemical shift imaging at 3 T. *Mult Scler* 17:289–96

Dixon CE, Clifton GL, Lighthall JW, Yaghmai AA, Hayes RL (1991) A controlled cortical impact model of traumatic brain injury in the rat. *J Neurosci Methods* 39: 253–62

Garnett MR, Blamire AM, Rajagopalan B, Styles P, Cadoux-Hudson TA (2000) Evidence for cellular damage in normal-appearing white matter correlates with injury severity in patients following traumatic brain injury: a magnetic resonance spectroscopy study. *Brain* 123(Pt 7): 1403–9

Gasparovic C, Yeo R, Mannell M, Ling J, Elgie R, Phillips J, Doezema D, Mayer AR (2009) Neurometabolite concentrations in gray and white matter in mild traumatic brain injury: an 1H-magnetic resonance spectroscopy study. *J Neurotrauma* 26:1635–43

Govind V, Gold S, Kaliannan K, Saigal G, Falcone S, Arheart KL, Harris L, Jagid J, Maudsley AA (2010) Whole-brain proton MR spectroscopic imaging of mild-to-moderate traumatic brain injury and correlation with neuropsychological deficits. *J Neurotrauma* 27:483–96

Gruetter R (1993) Automatic, localized *in vivo* adjustment of all first- and second-order shim coils. *Magn Reson Med* 29:804–11

Hall ED, Bryant YD, Cho W, Sullivan PG (2008) Evolution of post-traumatic neurodegeneration after controlled cortical impact traumatic brain injury in mice and rats as assessed by the de Olmos silver and fluorojade staining methods. *J Neurotrauma* 25:235–47

Holshouser BA, Tong KA, Ashwal S, Oyoyo U, Ghamsary M, Saunders D, Shutter L (2006) Prospective longitudinal proton magnetic resonance spectroscopic imaging in adult traumatic brain injury. *J Magn Reson Imaging* 24:33–40

Imbrosci B, Mittmann T (2011) Functional consequences of the disturbances in the GABA-mediated inhibition induced by injuries in the cerebral cortex. *Neural Plast* 2011:614329

Lei H, Berthet C, Hirt L, Gruetter R (2009) Evolution of the neurochemical profile after transient focal cerebral ischemia in the mouse brain. *J Cereb Blood Flow Metab* 29:811–9

Lescot T, Fulla-Oller L, Po C, Chen XR, Puybasset L, Gillet B, Plotkine M, Meric P, Marchand-Leroux C (2010) Temporal and regional changes after focal traumatic brain injury. *J Neurotrauma* 27:85–94

Loane DJ, Faden AI (2010) Neuroprotection for traumatic brain injury: translational challenges and emerging therapeutic strategies. *Trends Pharmacol Sci* 31:596–604

Lubin JH, Colt JS, Camann D, Davis S, Cerhan JR, Severson RK, Bernstein L, Hartge P (2004) Epidemiologic evaluation of measurement data in the presence of detection limits. *Environ Health Perspect* 112:1691–6

Marino S, Ciurleo R, Bramanti P, Federico A, De Stefano N (2011) 1H-MR spectroscopy in traumatic brain injury. *Neurocrit Care* 14:127–33

Markgraf CG, Clifton GL, Moody MR (2001) Treatment window for hypothermia in brain injury. *J Neurosurg* 95:979–83

Moffett JR, Tieman SB, Weinberger DR, Coyle JT, Namboodiri AM (eds) (2006) *N-Acetylaspartate: A Unique Neuronal Molecule in the Central Nervous System*. New York, NY: Springer

Pfeuffer J, Tkac I, Provencher SW, Gruetter R (1999) Toward an *in vivo* neurochemical profile: quantification of 18 metabolites in short-echo-time (1)H NMR spectra of the rat brain. *J Magn Reson* 141:104–20

Pleasant JM, Carlson SW, Mao H, Scheff SW, Yang KH, Saatman KE (2011) Rate of neurodegeneration in the mouse controlled cortical impact model is influenced by impactor tip shape: implications for mechanistic and therapeutic studies. *J Neurotrauma* 28:2245–62

Provencher SW (1993) Estimation of metabolite concentrations from localized *in vivo* proton NMR spectra. *Magn Reson Med* 30:672–9

Rice ME, Russo-Menna I (1998) Differential compartmentalization of brain ascorbate and glutathione between neurons and glia. *Neuroscience* 82:1213–23

Righi V, Roda JM, Paz J, Mucci A, Tugnoli V, Rodriguez-Tarduchy G, Barrios L, Schenetti L, Cerdan S, Garcia-Martin ML (2009) 1H HR-MAS and genomic analysis of human tumor biopsies discriminate between high and low grade astrocytomas. *NMR Biomed* 22:629–37

Saatman KE, Creed J, Raghupathi R (2010) Calpain as a therapeutic target in traumatic brain injury. *Neurotherapeutics* 7:31–42

Schafer JL (1997) *Analysis of Incomplete Multivariate Data*. Chapman & Hall: London

Schuhmann MU, Stiller D, Skardelly M, Bernarding J, Klinge PM, Samii A, Samii M, Brinker T (2003) Metabolic changes in the vicinity of brain contusions: a proton magnetic resonance spectroscopy and histology study. *J Neurotrauma* 20:725–43

Shutter L, Tong KA, Holshouser BA (2004) Proton MRS in acute traumatic brain injury: role for glutamate/glutamine and choline for outcome prediction. *J Neurotrauma* 21:1693–705

Signoretti S, Marmarou A, Tavazzi B, Dunbar J, Amorini AM, Lazzarino G, Vagnozzi R (2004) The protective effect of cyclosporin A upon N-acetylaspartate and mitochondrial dysfunction following experimental diffuse traumatic brain injury. *J Neurotrauma* 21:1154–67

Soblosky JS, Matthews MA, Davidson JF, Tabor SL, Carey ME (1996) Traumatic brain injury of the forelimb and hindlimb sensorimotor areas in the rat: physiological, histological and behavioral correlates. *Behav Brain Res* 79:79–92

Tavazzi B, Signoretti S, Lazzarino G, Amorini AM, Delfini R, Cimatti M, Marmarou A, Vagnozzi R (2005) Cerebral oxidative stress and depression of energy metabolism correlate with severity of diffuse brain injury in rats. *Neurosurgery* 56:582–9; discussion -9

Tkac I, Rao R, Georgieff MK, Gruetter R (2003) Developmental and regional changes in the neurochemical profile of the rat brain determined by *in vivo* 1H NMR spectroscopy. *Magn Reson Med* 50:24–32

Tkac I, Starcuk Z, Choi IY, Gruetter R (1999) *In vivo* 1H NMR spectroscopy of rat brain at 1 ms echo time. *Magn Reson Med* 41:649–56

Vagnozzi R, Signoretti S, Cristofori L, Alessandrini F, Floris R, Isgro E, Ria A, Marziale S, Zoccatelli G, Tavazzi B, Del Bolgia F, Sorge R, Broglio SP, McIntosh TK, Lazzarino G (2010) Assessment of metabolic brain damage and recovery following mild traumatic brain injury: a multicentre, proton magnetic resonance spectroscopic study in concussed patients. *Brain* 133:3232–42

Xing G, Ren M, O'Neill JT, Verma A, Watson WD (2012) Controlled cortical impact injury and craniotomy result in divergent alterations of pyruvate metabolizing enzymes in rat brain. *Exp Neurol* 234:31–8

Xu S, Zhuo J, Racz J, Shi D, Roys S, Fiskum G, Gullapalli R (2011) Early microstructural and metabolic changes following controlled cortical impact injury in rat: a Magnetic Resonance Imaging and Spectroscopy Study. *J Neurotrauma* 28:2091–102

Yokobori S, Watanabe A, Matsumoto G, Onda H, Masuno T, Fuse A, Kushimoto S, Yokota H (2011) Time course of recovery from cerebral vulnerability after severe traumatic brain injury: a microdialysis study. *J Trauma* 71:1235–40

Zacharoff L, Tkac I, Song Q, Tang C, Bolan PJ, Mangia S, Henry PG, Li T, Dubinsky JM (2012) Cortical metabolites as biomarkers in the R6/2 model of Huntington's disease. *J Cereb Blood Flow Metab* 32:502–14

Zhao X, Ahram A, Berman RF, Muizelaar JP, Lyeth BG (2003) Early loss of astrocytes after experimental traumatic brain injury. *Glia* 44:140–52

Zhou J, Neale JH, Pomper MG, Kozikowski AP (2005) NAAG peptidase inhibitors and their potential for diagnosis and therapy. *Nat Rev Drug Discov* 4:1015–26